HTD-Vol. 263

ENHANCED COOLING TECHNIQUES FOR ELECTRONICS APPLICATIONS

presented at
The 1993 ASME Winter Annual Meeting
New Orleans, Louisiana
November 28 - December 3, 1993

sponsored by
The Heat Transfer Division, ASME

edited by
S. V. Garimella
University of Wisconsin - Milwaukee

M. Greiner
University of Nevada - Reno

M. M. Yovanovich
University of Waterloo

V. W. Antonetti
Manhattan College

THE AMERICAN SOCIETY OF MECHANICAL ENGINEERS
UNITED ENGINEERING CENTER / 345 EAST 47TH STREET / NEW YORK, NEW YORK 10017

HTD-Vol. 263, Enhanced Cooling Techniques
for Electronics Applications
ASME 1993

CONDUCTION HEAT TRANSFER MEASUREMENTS FOR AN ARRAY OF SURFACE MOUNTED HEATED COMPONENTS

M. Arabzadeh, E. L. Ogden, and A. J. Ghajar
School of Mechanical and Aerospace Engineering
Oklahoma State University
Stillwater, Oklahoma

ABSTRACT

An experimental investigation was conducted to examine the effect of varying Reynolds number, component placement, and board conductivity on the conduction heat transfer to the board, component temperature, and heat transfer coefficient. Experiments were conducted in a horizontal rectangular wind tunnel using an array of twelve components placed in four rows and three columns. All components were made out of polished aluminum cubes and each component was individually powered with a resistor element. The heat flux and temperature were measured on all sides of the middle heated components in each row of the array by a direct measurement heat flow sensor equipped with a thermocouple. The heat transfer by conduction through the back of the board was measured directly beneath and surrounding the heated components. The experimental results indicate that the conduction heat transfer through the board and consequently the thermal behavior of the system were strongly affected by the Reynolds number of the flow, placement of the component, and the board conductivity. For the experiments conducted in this study, heat transfer by conduction accounted for 1 to 91% of the total power applied to the component and the component temperature varied from 25 to 132°C.

NOMENCLATURE

A_C	total exposed surfaces of the heated component
D	height of the rectangular channel
h	convection heat transfer coefficient of the heated component
h_a	actual convection heat transfer coefficient of the heated component
h_c	calculated convection heat transfer coefficient of the heated component
H	height of flow passage between the component and opposite wall of the channel
k	thermal conductivity
L	component planform dimension
Q_c	rate of convection heat transfer for the heated component
Q_k	total conduction loss of the heated component
Q_r	thermal radiation of the heated component to the surroundings
Q_t	input power to the heated component
Re	Reynolds number based on H = 2L, $H\bar{V}/\nu$
S	intercomponent spacing
t	height of component
T_C	average temperature of the exposed surfaces of the heated component
T_∞	temperature of approach air upstream of the test section
V	channel local air velocity
$\bar{V}$	channel average air velocity
V_{max}	air velocity at the center of the channel
y	normal spatial coordinate
ν	kinematic viscosity of air at T_∞

INTRODUCTION

Technological advances have produced microminiaturized integrated circuits with very high electronic component densities and correspondingly large cooling heat flux requirements. Heat transfer thus has become an extremely important consideration in the design of the high speed digital electronics which are at the forefront of modern engineering and science research and development. The design of computer systems with acceptable reliability requires accurate prediction of

component operating temperatures. Accurate prediction of component temperature depends on the heat transfer coefficient which, in turn, is influenced by the conduction heat transfer to the board.

An extensive review of the literature pertinent to convective cooling of electronic boards have been compiled by Incropera (1988). Most previous investigators did not adequately address the problem of conduction , since they tried to minimize the conduction effects by using insulating materials. This kept the problem simple and tractable, and made it possible to do well controlled experiments and simple analyses. There has been no systematic attempt to study and incorporate the effect of conduction in a circuit board. Because the majority of the heat is ultimately removed through convection, the effects of conduction are often overlooked. If conductive board is used, the problem will be more complex, since the conduction coupling between the components and the board can represent a significant thermal path for dissipation of heat. This was the main purpose of this study.

Wagner (1984) used epoxy-glass board with different thick layers of copper in order to investigate effects of board conductivity on temperature distribution on the back of the board. A heat source of low power (1.0 W) was placed at the center of the board to represent a silicon integrated chip. Conduction losses were calculated rather than being directly measured. The experiments were performed with only one low velocity (1.0 m/s), therefore effects of different Reynolds numbers were not investigated.

Ortega (1986) used a board consisting of balsa wood epoxied onto plexiglas in an effort to minimize conduction heat transfer through the board. Ortega and Kabir (1991) also used balsa wood mounted on plexiglas for the board. Kang et al. (1990) tried to limit conduction by using three masonite boards separated by 6 mm air gaps. Roeller et al. (1990) used a thermally symmetric channel design on a cardboard board to minimize conduction heat transfer through the board.

Studies using convection in fluids other than air generally had insignificant amounts of conduction. For example, Garimella and Eibeck (1990) estimated that the conduction for their setup cooled by forced convection in water accounted for less than 1% of the total heat dissipated.

Some investigators have attempted to account for conduction by numerical or analytical methods. Laderman et al. (1987) conducted a numerical study of several conduction heat transfer schemes and examined the sensitivity of the component junction and board temperatures to certain parameters which affect conduction.

Some studies effectively correlated models with experimental results. Fitch (1990) proposed a model using a thermal resistance network which included the effects of conduction. Experiments were also conducted and the temperatures were found to correlate well with the proposed model.

Ortega and Kabir (1991) developed an analytical model for the conduction from a component to the board. This model suggested that conduction varies linearly with a modified driving temperature. This model correlated well with experimental conduction flux data calculated from thermocouple temperatures within the component.

Manno and Azar (1991) examined the effect of intercomponent coupling which included conduction and radiation. All the correlations which were examined underpredicted component temperatures. They note that this is potentially due to underestimating conduction losses. They conclude that the non-convective mechanisms, which consist mainly of conduction, account for approximately 34% of the total heat dissipated from a powered component.

Some experimenters have examined the influence of conduction on certain quantities. Azar and Moffat (1991) studied the effect of conduction on the heat transfer coefficient. Only the convective flux from the top of the component was experimentally measured using a heat flux sensor. They assumed that the convective heat flux from the other surfaces of the component (front, back, and sides) is equal to the heat flux from the top (as will be shown, not a particularly good assumption). Employing this assumption, from an energy balance, they determined the total conductive heat flux of the component. Conduction percentages between 24.3% and 60.0% were reported.

While there has been considerable interest in the effect of conduction, there has not been a systematic attempt to experimentally determine the influence of varying Reynolds number, component placement, and board conductivity on the conduction heat transfer to the board, component temperature, and heat transfer coefficient. The objective of this study was to conduct such experiments in a horizontal rectangular wind tunnel using polished aluminum cubes to simulate electronic components.

EXPERIMENTAL SETUP AND PROCEDURES

A schematic diagram of the apparatus used in the experiments is shown in Fig. 1. The test components were mounted along the top wall of a 1.52 m long rectangular duct with a fixed 25.4 cm width and a height that was easily adjustable from 1.27 to 7.62 cm. The rectangular duct was constructed of 1.27 cm commercial grade plexiglas. Ambient air entered the rectangular duct through a 101 cm long wooden contraction which was designed to provide smooth flow of entering air. The movable bottom section was easily adjusted to accommodate any channel height between 1.27 and 7.62 cm. The inlet to outlet ratio (contraction ratio) varied from 14.5 to 82, depending on the channel height. The flow straightener at the entrance to the rectangular duct provided a uniform velocity profile. The flow straightener (0.678 open area ratio) consisted of soda straws (0.55 cm

inside diameter, 12 cm length) tightly packed between galvanized steel mesh screens (0.044 cm wire diameter, 0.32 cm mesh width). The rectangular duct consisted of three sections: a 68.6 cm entrance section, a 53.3 cm test section, and a 30.5 cm exit section. The test section was designed such that its upper wall could be removed and reset in place quickly, thus enabling rapid access to the array of components. The start of the test component array was positioned 78.5 cm from the entrance to the duct and extended for 12.45 cm downstream. Ambient air was drawn past the test components by a 2 HP variable speed blower mounted downstream of the rectangular duct. The duct emptied to an acoustically absorbent plenum that served to isolate the test flow from the blower noise. The air velocity was measured and adjusted (via a computer controlled damper/stepper motor arrangement) in the round duct between the plenum and the blower by an MKS model 223BD differential pressure transducer and a pitot static tube. The blower was mounted within an insulated box and exhausted outside the building, allowing flow visualization experiments with smoke to be performed (Wang and Ghajar, 1991).

Electronic chips were modeled by highly polished aluminum cubes (2.54 cm per side) with a thermal conductivity of 216.3 W/m-K. The components were heated using resistance heating. Each component was equipped with a 475 ohm ceramic resistor placed at the center of the component (see Fig. 2). The rest of the cavity in the back of the block was filled with Omegabond 101 thermally conductive epoxy.

The components were arranged in an array with four rows in the streamwise direction and three columns in the cross-stream direction (see Fig. 3). The dimensionless length ratios which define the geometrical characteristics of the array are:

$$t/L = 1 \; ; \; S/L = 0.3 \; ; \; (H+t)/L = 3$$

The difference between component height and channel height (H = D - t = 2L), is the characteristic length used for calculation of the Reynolds number. Components were oriented such that the lead wires through which current is supplied to the resistor emerge from the downstream side of the cube. These wires were secured against the board and followed the board to the end of the test section where they emerged from the air channel via holes sealed with putty.

The test board on which the array of components was mounted, was positioned in the test section in place of the plexiglas ceiling. It occupies the entire width and length of the test section and rests flush with the ceiling of the rest of the channel. Three boards of different materials were used. The materials were chosen in order to have a significant variation in thermal conductivity. The materials chosen were fiberglass (0.160 cm thick) with a thermal conductivity of 0.293 W/m-K, aluminum 2219 alloy (0.155 cm thick) with a thermal conductivity of 130 W/m-K, and balsa wood (0.645 cm thick) with a thermal conductivity of 0.07 W/m-K.

The power delivered to each component was computer controlled. The present power controller system can

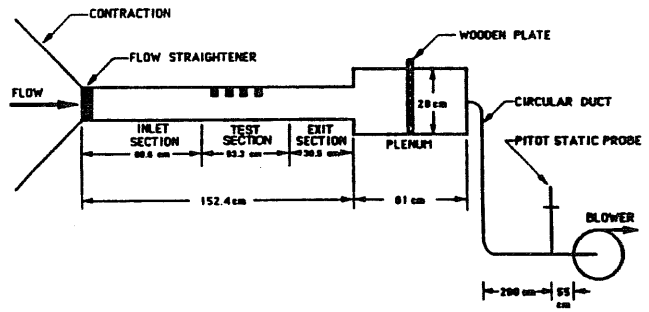

Figure 1. Schematic of Experimental Apparatus.

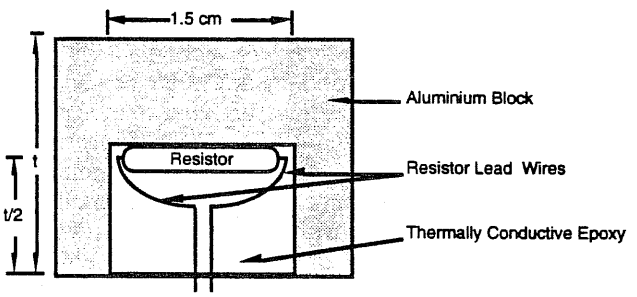

Figure 2. Detail of a Heated Component.

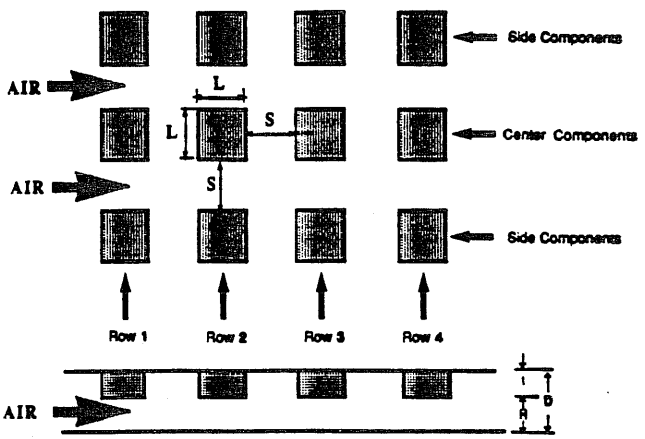

Figure 3. Top and Side Views of the Inline Arrangement of the Components in the Test Section.

handle up to forty-eight components and the power delivered to each component can be individually varied from 0 to 5 W in increments of 0.1 W. The power controller unit has a microcomputer which controls the switching circuitry and communicates via a serial port to a personal computer. Calibration tests for this unit providing different power for each component has been performed while monitoring supplied powers with an accurate oscilloscope. The tests showed that the power

controller unit works with an accuracy of ±1% of the delivered power.

The heat flux and temperature on all five exposed surfaces (inside the wind tunnel) and the back of the board (outside of the wind tunnel) for the middle heated components in each row of the array were measured by a direct measurement heat flow sensor equipped with a built-in T-type thermocouple (RdF corporation, model 20453-3). These sensors were 1.27 cm square, and placed exactly at the center of heated component surface using Omegatherm 201 a very high thermally conductive silicon paste. Each heat flow sensor was individually calibrated at a base temperature of 21°C with output of 5.83×10^{-8} Vm^2/W, thermal resistance of 2.11×10^{-3} °C m^2/W, heat capacity of 1022 J/m^2-°C, and response time of 0.400 seconds. It is important to note that these sensors measure radiation as well as convection losses. For monitoring the heat flux on all sides of the components, the voltage signals from the heat flux sensors were passed through a high gain DC amplifier. The output of the amplifier was then connected to a personal computer equipped with an A/D board. Estimates of uncertainty of the measured heat fluxes with negligible thermal contact resistance between the module and the board was determined to be ±5% (Kline and McClintock, 1953). This estimate of uncertainty increased to about 16% when an estimate of the maximum possible value of thermal contact resistance for the experiments was included in the uncertainty analysis.

To relate velocity measurements in the duct to the inlet mean velocity of the air at the entrance to the test section, extensive measurements at both locations were conducted. These measurements consisted of traversing the circular duct and the rectangular channel by a pitot static tube and then numerically integrating the local velocities to obtain the mean velocity at each location. These measurements were conducted for several air velocities ranging from 2 to 12 m/s. From these measurements and the application of conservation of mass between the two locations, correlations which relate velocity measurements at the center of the duct to the mean air velocity at the inlet to the test section were developed. The mean air velocity at the inlet to the test section calculated from the developed relationships were compared with actual measurements for several different velocities. The calculated values in all instances were within ±2% of the measurements. Estimates of uncertainty (Kline and McClintock, 1953) show the uncertainty in the mean channel inlet air velocity varies from ±0.65%, at high velocities, to ±6.7%, at low velocities.

To verify flow uniformity in the test section, the velocity profiles just upstream and downstream of the test section were measured with a pitot static tube and a differential pressure transducer. These measurements were made at three different locations across the width of the channel (at channel center line and about 6 cm from the wall on either side of the channel center line) and up to fifteen locations (depending on the channel height) across the height of the channel. Velocity profiles for different flow settings at different locations indicated reproducible, uniform, and symmetric velocity profiles. Figure 4 shows a typical velocity profile for the experiments. The results presented in this figure are for a channel height of 7.62 cm and the velocity profiles were obtained at three different locations across the width of the channel just upstream and downstream of the test section (68 cm and 122 cm from the entrance to the rectangular duct).

Table 1. Data Taken for Each Case and Board Material*

Case	Power Supplied to the Middle Components (Watts)	Fiberglass Board	Aluminum Board	Balsa Wood Board
1	1	I,T,S,F,B,C,EB,L	I,T,S,F,B,C,EB,L	I,C
2	3	I,T,S,F,B,C,EB,Re	I,T,C	I,C
3	4.5	I,T,S,F,B,C,EB,L,Re	I,T,S,F,B,C,EB,L,Re	I,T,C,Re

I = inlet air temperature
T = flux and temperature for the top of the component
S = flux and temperature for the side of the component
F = flux and temperature for the front of the component
B = flux and temperature for the back of the component
C = flux and temperature for the bottom of the board
EB = an energy balance was performed
L = lateral conduction from the back of the board was measured
Re = flux and temperature for the bottom of the board was taken for eight Reynolds numbers ranging from 1450 to 30400

* Unless otherwise specified all data was taken at a Reynolds number of 3800

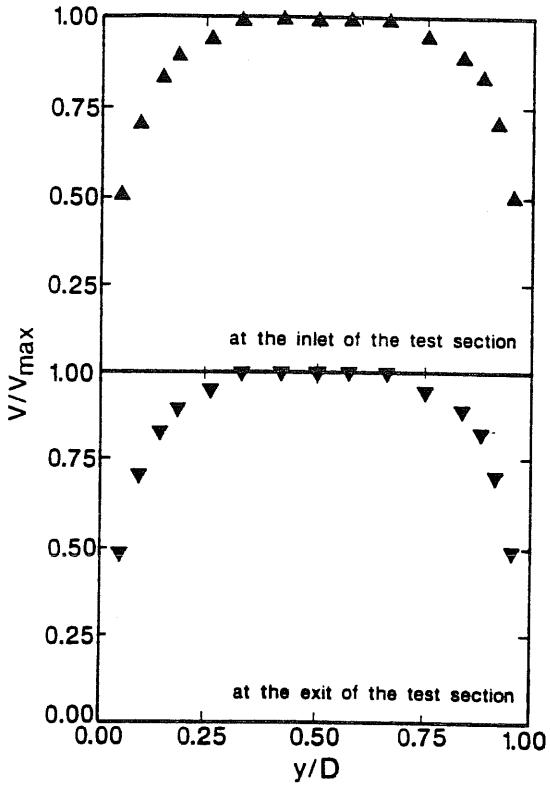

Figure 4. Dimensionless Velocity Profile at the Inlet and Exit of the Test Section.

RESULTS AND DISCUSSION

Table 1 summarizes the experiments that were conducted to show the influence of varying Reynolds number, component placement, and board conductivity on conduction heat transfer to the board, component temperature, and heat transfer coefficient. The data were collected for the middle heated components of an array of twelve components placed in four rows (stream-wise) and three columns. During the data collection all of the center components were heated simultaneously. Table 1 summarizes the three different power distributions (referred to as cases) that were used for the experiments. This table gives a summary of the specific data taken for each case using each of the three boards. As indicated in Table 1, the Reynolds number based on the difference between component height and channel height (H), was either 3800 or varied from 1450 to 30400.

When examining the results, it must be kept in mind that there will be irregularities due to the exposure of the first and last rows. The first row will lose a disproportionate amount of heat through its front surface (the surface facing the air flow) due to the increased air velocity over that surface. Similarly, the fourth (last) row will lose more heat through its back surface than other components due to its exposure. These losses will affect the remaining sides.

Conduction heat flux for each of the heated components is directly measured beneath the component on the back of the board (outside of the wind tunnel), using a heat flux sensor. This value will be referred to as the "direct conduction". Direct conduction is not the total conduction heat transfer from the heated component. A large portion of the heat (depending on the board conductivity) will be dissipated by conduction from the surface of the board both inside and outside of the channel in all directions around the bottom of the heated component. This will be referred to as the "lateral conduction". As mentioned before, the readings from heat flow sensors for the five exposed surfaces were the sum of convective and radiative heat fluxes. Subtracting this total convective and radiative heat transfer from the input power to the component, gives the "total conduction" heat transfer. Dividing the "direct conduction", and the "total conduction" by the input power to the heated component, gives the "direct conduction percentage", and the "total conduction percentage", respectively. The difference between the total and direct conduction is the lateral conduction. Efforts were made to account for the lateral conduction by direct measurements. In order to accomplish this, experiments were performed with a single heated component placed 91.5 cm from the entrance of the rectangular channel on two different boards, a 0.155 cm thick aluminum board, and a layer of 0.16 cm thick fiberglass board placed on a 1.27 cm thick commercial plexiglas. The back of the board (outside of the wind tunnel) was divided into uniform grids of the size 1.27 cm x 1.27 cm, same size as the heat flux sensors, up to a distance of 5L around the component. Conduction heat flux and temperature of each individual grid was carefully measured by the heat flux sensors. Two different input powers (1 and 4.5 W) and several different air velocities ranging from 2 to 12 m/s were used. These detailed measurements revealed that it is not possible to account for all of the lateral conduction, since part of the heat is dissipated by conduction from the inside part of the board around the component.

Figure 5(a) shows one of these grid systems used to measure the local conduction heat fluxes from the back of the aluminum board around the component in terms of mW, and temperature above T_∞ in °C, for a fixed 4.5 W input power to the component and 7.5 m/s channel average air velocity. Bottom of the heated component is highlighted in Fig. 5(a) by the thick lines. The top number shown inside of each grid is the local temperature above T_∞ in °C, while the bottom number is the local conduction heat flux in mW. It was assumed that the heat flux and temperature distributions about the component center-line were symmetric in the streamwise direction. This assumption was applied to those grids that their heat flux and temperature were not directly measured. However, this symmetric assumption can not be made about the component center-line in the spanwise direction,

0.78 5.26						1.00 5.42	1.00 5.42						0.89 6.59
						1.06 5.93	1.06 5.93						
						1.44 6.09	1.44 6.09						
						1.5 6.5	1.5 6.5						
						1.61 7.2	1.61 7.2						
						1.94 7.4	1.94 7.4					1.56 7.1	
		1.67 8.3	2.00 8.7	1.28 7.1	2.28 8.9	2.17 8.2	2.17 8.2	2.28 8.9	1.28 7.1	2.00 8.7	1.67 8.3		
		1.67 8.3	2.17 9.0	2.17 7.6	2.78 9.6	2.67 9.6	2.67 9.6	2.78 9.6	2.17 7.6	2.17 9.0	1.67 8.3		
		2.11 9.1	2.44 9.4	2.61 10.1	3.11 11.2	3.33 10.2	3.33 11.0	3.11 11.2	2.61 10.1	2.44 9.41	2.11 9.1		
		2.39 9.1	2.72 9.9	3.06 11.2	3.61 10.3	4.44 13.1	4.56 15.7	3.94 14.2	3.06 11.2	2.72 9.9	2.39 9.1		
1.67 6.1	1.94 6.1	2.22 7.0	2.67 6.9	3.06 7.6	3.78 8.7	**5.11** **13.2**	**6.00** **19.2**	4.72 14.3	3.61 10.7	2.94 9.4	2.50 8.4	2.00 7.4	1.83 7.3
1.67 6.1	1.94 6.1	2.22 7.0	2.67 6.9	3.06 7.6	3.78 8.7	**5.28** **16.5**	**6.06** **16.7**	4.67 12.6	3.61 10.4	2.89 9.1	2.39 8.2	1.94 7.6	1.83 7.8
		2.2 7.5	2.07 8.0	1.94 8.4	3.00 8.6	4.56 8.1	4.56 8.1	3.00 8.6	1.94 8.4	2.07 8.0	2.2 7.5		
		2.08 7.2	1.98 7.4	1.67 7.4	2.72 7.3	3.39 6.8	3.39 6.8	2.72 7.3	1.67 7.4	1.98 7.4	2.08 7.2		
		2.17 7.9	2.11 7.5			2.83 6.6	2.83 6.6			2.11 7.5	2.17 7.9		
		1.94 7.4	1.83 7.4			2.17 6.0	2.17 6.0			1.94 7.4	1.83 7.4		
						1.89 5.8	1.89 5.8						
0.167 5.2						1.61 6.3	1.61 6.3						0.22 5.3

↑
Air Flow

Figure 5(a). Local Temperatures Above T_∞ in °C (top numbers in the grids), and Local Conduction Losses in mW (bottom numbers) Around the Heated Component on the Back of the Aluminum Board.

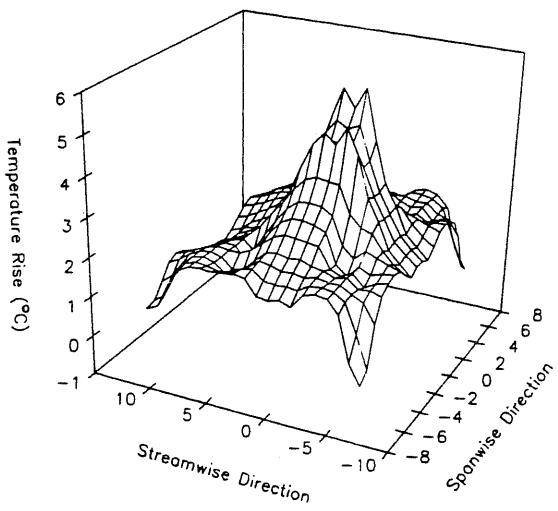

Figure 5(b). Variation of Local Temperature Above T_∞ Around the Heated Component on the Back of the Aluminum Board.

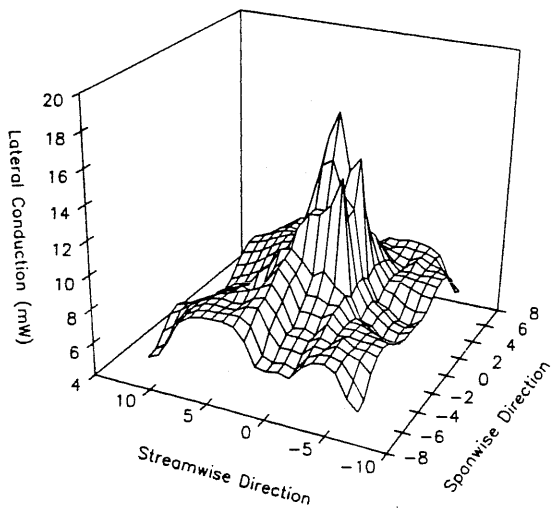

Figure 5(c). Variation of Local Conduction Loss Around the Heated Component on the Back of the Aluminum Board.

because of the thermal wake effect upstream of the component due to the air flow. The variations of temperature rise above T_∞ and the lateral conduction in the streamwise and spanwise directions given in Fig. 5(a) are depicted in two distinct 3-D plots in Figs. 5(b) and 5(c). Adding all of these local conduction heat fluxes gives 1.079 W. Measured convective and radiative heat fluxes from the exposed surfaces through the sensors were 0.161, 0.182, 0.173, 0.173, and 0.128 W from the top, front, left side, right side, and back of the component, respectively. Adding these values and subtracting from 4.5 W input power, gives 3.683 W which should be the total conduction loss. However, total measurement of the conduction loss from the back of the board up to 5L around the component (from Fig. 5) was only 1.079 W. This value was 0.241 W for the fiberglass board for the same input power and channel average air velocity, while the total conduction obtained from the energy balance was 0.469 W. From this comparison, it seems that the correct way to account for the total conduction heat transfer is to use an energy balance by subtracting the total measured convective and radiative heat fluxes of the exposed surfaces from the input power to the component.

Effect of Board Conductivity

The amount of conduction losses can greatly affect the component operating temperature and therefore the reliability of the system as a whole. In this study, conduction was controlled by changing board material. Boards with different thermal conductivities allowed different amounts of conduction. Balsa wood with a low thermal conductivity (0.07 W/m-K) was used to minimize conduction, while aluminum with a high thermal conductivity (130 W/m-K) was used to maximize conduction.

Figure 6 shows the temperature rise of the middle components for case 3 using three different boards. The different board conductivities had a large effect upon the component temperature rise. In other words, with a fixed input power to the component, the higher conductive board has more conduction heat transfer through the back of the board and less convection and radiation through the exposed surfaces, hence less component temperature rise. For example, the temperature rise of the heated component at row 1 was 13°C, 40.5°C, and 50°C for the aluminum, fiberglass, and balsa wood, respectively. Similarly, these temperature rises for row 4 were 16°C, 60.2°C, and 80°C for the three respective boards. The difference in temperature rise is very significant when a 10°C increase is considered to double the component failure rate (Weiss et al., 1989). This figure also reveals the hydrodynamic and thermal effects of upstream components on the temperature rise of downstream components, since all of the middle components were heated simultaneously. As mentioned earlier, there are some irregularities due to the exposure of the last row. It is recommended that the component with higher power be placed in row 1 in electronic packaging, since its operating temperature will be lower, thereby providing higher reliability.

Figures 7 and 8 complement the results shown in Fig. 6. Figure 7 shows the effect of board conductivity on the total conduction percentage of the heated component at row 3 for case 3 with different Reynolds numbers, while Fig. 8 depicts effect of board conductivity on component temperature rise at row 3 for case 3 with different Reynolds numbers. Comparing Figs. 6 and 7 for a fixed Reynolds number of 3800 and input power of 4.5 W, the component temperature rise at row 3 is 17°C, 65.6°C, and 77°C (see Fig. 6), while the total conduction percentage is 89%, 21%, and 6% (see Fig. 7) for the aluminum, fiberglass, and balsa wood boards, respectively. It is important to note that with a fixed Reynolds number, the board with the higher thermal conductivity, dissipates more heat through the back of the board by conduction (see Fig. 7), rather than by convection and radiation through the exposed surfaces, which in turn, causes less temperature rise of the heated component (see Figs. 6 and 8). Figure 7 also shows that the total conduction percentage decreases with increasing Reynolds number. For example, for a Reynolds number of 1470, the total conduction percentage is 91%, 26.7%, and 7.2%, while for a Reynolds number of 30450, the total conduction percentage is 78.3%, 5%, and 1.2% for the aluminum, fiberglass, and balsa wood boards, respectively. Higher Reynolds number means faster air movement around the exposed surfaces of the component causing more heat dissipation by convection and less by conduction. This increase in convection heat transfer reduces the operating temperature of the heated component as can be seen in Fig. 8. The temperature rise for the balsa wood board was 110°C at the lowest Reynolds number. This was 28°C higher than that for the fiberglass board. The temperature rise for the fiberglass board was in turn, 57°C higher than that for the aluminum board. At high Reynolds number, the temperature rise for the balsa wood board was only 1°C higher than that for the fiberglass board. However, the temperature rise for the fiberglass board was 10°C higher than that for the aluminum board.

The role of board conductivity on direct and lateral conduction losses can be further analyzed by revisiting the data of Fig. 7. If for this data "lateral conduction" contributions are ignored and only "direct conduction" effects are considered, the results will appear as Fig. 9. Comparison of Figs. 9 and 7 show that conduction percentage for aluminum is less than fiberglass and balsa wood for the same operating conditions. This is obviously not true. As discussed earlier, a great portion of conduction heat transfer for a conductive board (aluminum) is by lateral conduction, while for a relatively non-conductive board (balsa wood) this portion is very small. For example, for a fixed Reynolds number of 1470, the direct conduction percentage is 4%, 16.5%, and 6.5%, while the total conduction percentage is 91%, 26.7%, and 7.2% for the aluminum, fiberglass, and balsa

wood boards, respectively. This means that heat transferred by lateral conduction is 87% for aluminum, 10.2% for fiberglass, and only 0.7% for balsa wood board.

The effects of board conductivity and Reynolds number on conduction losses are not addressed as a major contribution to the heat transfer in most of the works done in electronic cooling. This is perhaps because most of those measurements were conducted at higher Reynolds numbers regimes using nonconductive board. In fact, this is also shown in this study on Fig. 7 for Reynolds numbers above 10,000 (total conduction percentage is less than 9 for balsa wood and fiberglass board). Results of this work could become more useful if more measurements are performed for a set of lower Reynolds numbers. A correlation may be obtained between the percentage of conduction losses and Reynolds numbers for a range of Reynolds numbers below 2000.

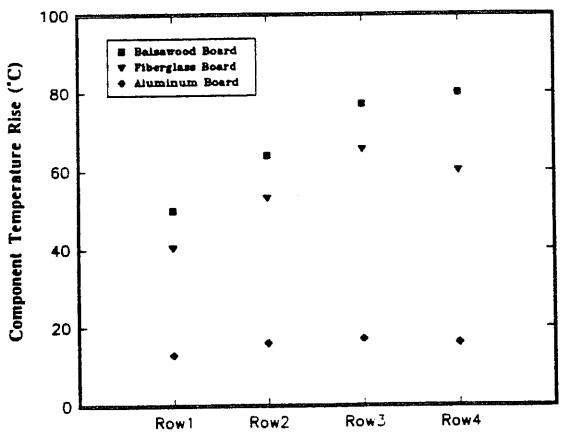

Figure 6. Effect of Board Conductivity on Component Temperature Rise for Different Component Placement of Case 3.

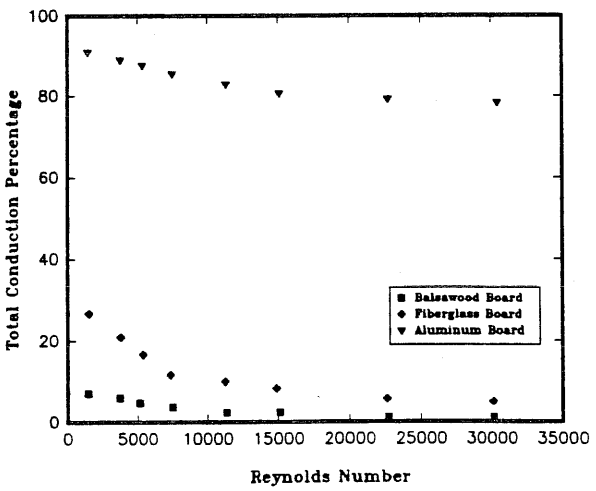

Figure 7. Effect of Board Conductivity on Total Conduction Percentage for Different Reynolds Numbers (Row 3 of Case 3).

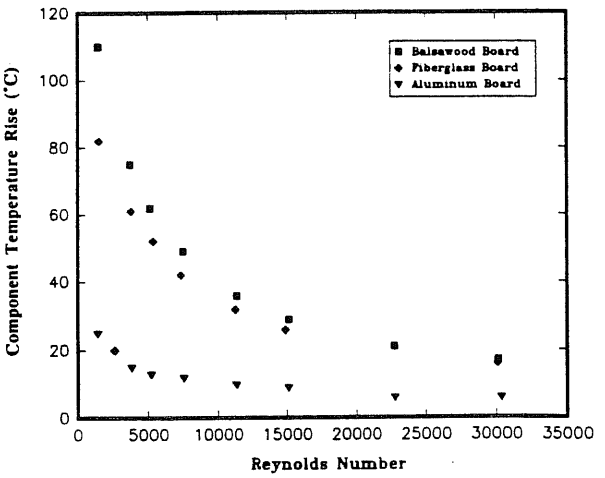

Figure 8. Effect of Board Conductivity on Component Temperature Rise for Different Reynolds Numbers (Row 3 of Case 3).

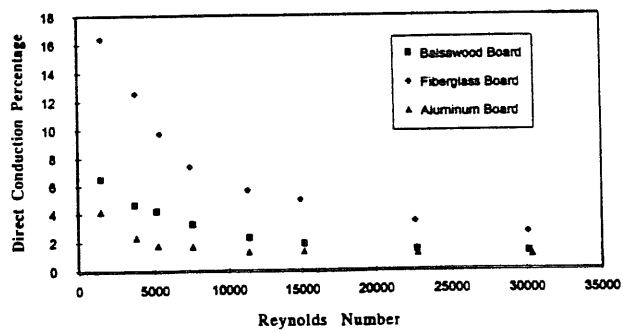

Figure 9. Effect of Board Conductivity on Direct Conduction Percentage for Different Reynolds Numbers (Row 3 of Case 3).

Influence of Conduction and Board Conductivity on the Heat Transfer Coefficient

The total rate of heat transfer from the exposed surfaces measured with the heat flow sensors by the experimenter, is the sum of convective and radiative heat transfers. The net rate of thermal radiation heat exchange between the surfaces and the surroundings (Q_r) can be calculated from Stefan-Boltzmann law, which in general is less than 3% of the total power supplied. Therefore, the experimenter can directly find the value of the convective heat transfer of the heated component (Q_c), then the value of the heat transfer coefficient (h) can be determined from:

$$h = Q_c/A_c\,(T_c - T_\infty) \qquad (1)$$

where A_c is the total exposed surfaces of the heated component, T_c is the average temperature of the exposed surfaces, and T_∞ is the approaching air temperature. Working with heat flux sensors is tedious, time consuming, and causes flow disturbance due to presence of exposed wires. Therefore, most of the experimenters preferred temperature measurements rather than using heat flow sensors. They found the convective heat transfer by employing an energy balance:

$$Q_c = Q_t - Q_k - Q_r \qquad (2)$$

where Q_t is the total input power to the component, and Q_k is the calculated conduction heat transfer using the board thermal conductivity. However, typically the industrial users directly apply the heat transfer coefficient offered by the experimenter in order to predict the operating temperature of the heated component:

$$T_c = T_\infty + (Q_c/hA_c) \qquad (3)$$

The actual heat transfer coefficient (h_a) can be found by using the correct measured value of total conduction loss in Eq. (2). However, almost all of the experimenters used one-dimensional calculated conduction loss in Eq. (2) in order to find the calculated heat transfer coefficient (h_c) from Eq. (1). Figure 10 shows comparison of these two values for the heated component at row 3 of case 3 for fiberglass board at different Reynolds numbers. This figure reveals that the calculated heat transfer coefficient is overestimated for all of the Reynolds numbers. The average difference between h_c and h_a is 7% with a maximum of 16% at the lowest Reynolds number. This difference would be higher if the board with higher conductivity is used, since the percentage of lateral conduction is higher which is not taken into account in the one-dimensional conduction loss calculation. An attempt was made to directly compare the heat transfer results of this study with the data in the literature. The arrays tested by previous investigators were different in size and geometry, as well as the material used for the board and simulated component(s). Hence, the results of these studies can not be directly compared with one another, as though to test for agreement or disagreement. However, Fig. 10 depicts a general comparison of the heat transfer results of this study with those experimenters who ignored lateral conduction loss and only considered one-dimensional calculated conduction loss using the board thermal conductivity.

In most practical applications of convective cooling in air, there will be some heat lost due to conduction. If the experimenter either ignores or underestimates these losses, then by employing Eqs. (2) and (1), Q_c and h will be overestimated. Use of this overestimated heat transfer coefficient by the industrial user, causes underprediction of the component operating temperature in Eq. (3). On the other hand, if the user uses the accurate value of h offered by the experimenter, but either ignores or underestimates the conduction losses, then Q_c in Eq. (2) will be overestimated, which in turn, causes overprediction of the component operating temperature in Eq. (3). While having the operating temperature lower than what predicted, is generally not a problem from the reliability aspect, it is preferable to predict the component operating temperature as accurately as possible. This important task can be accomplished by the correct estimation of the conduction losses.

The value of the conduction losses and the consistency between the experimenter and the industrial user in the way they estimated this value, plays a major

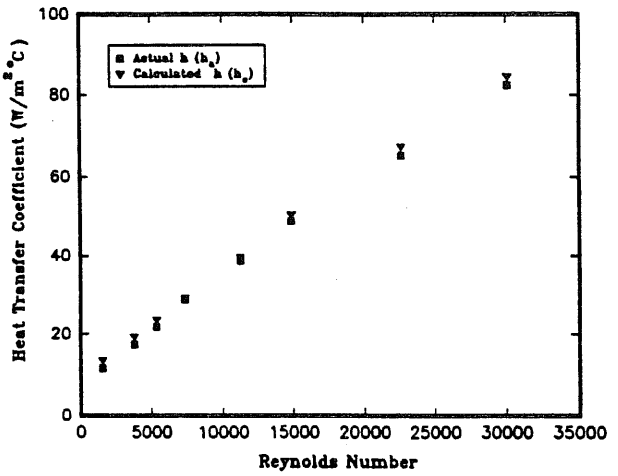

Figure 10. Comparison of Actual and Calculated Heat Transfer Coefficients for Different Reynolds Numbers (Row 3 of Case 3 for Fiberglass Board).

role in accurate prediction of the operating temperature, and it can cause serious problems if there is a failure of communication. Taking into account the accurate value of conduction losses, could allow greater packaging densities and therefore better overall circuit performance.

CONCLUSIONS

The objective of the present work was mainly to determine effects of conduction losses of the heated component and board conductivity, on the convection heat transfer coefficient and consequently on the operating temperature of the heated component. Experiments were performed with different board materials, each one arranged with an inline array of four rows by three columns of highly polished aluminum cubes, in a horizontal rectangular wind tunnel. Data were collected for different ranges of channel average air velocities, as well as input powers to the heated component. Results of this study reveals important specific conclusions:

1. Total conduction heat transfer of the heated component is the sum of two terms: "Direct Conduction" which is one-dimensional conduction and accounts for the amount of heat dissipated directly beneath the component on the back of the board, and "Lateral Conduction" which is what dissipated by conduction from all around the component either inside or outside surface of the board. Almost all of the previous investigators either completely ignored the total conduction, or only accounted for one-dimensional conduction, i.e. direct conduction. The error is significant, because this study shows that lateral conduction is generally higher than 50% of the total conduction. Ignoring this significant value, overestimates the heat transfer coefficient. This causes underprediction of the operating temperature of the chip by the industrial

user; hence, reduction in the overall reliability of the system.

2. Board conductivity can have significant direct effect on the operating temperature of the heated component. This study shows that the temperature rise of the heated component mounted on a conductive board such as aluminum is generally much less than what is for a relatively non-conductive board such as fiberglass or balsa wood board. However, in the electronic equipment, packages are mounted on the printing wiring board (PWB) where layers of electrical conductor networks are fabricated to connect the different packages. Hence, the material used for PWB should be electrically non-conductive. This causes a problem, since generally any heat conductive material is also electrically conductive and vice versa. More research should be conducted in this area to further quantify the influence of board material in order to find a suitable material to be able to transfer more heat by conduction and reduce the operating temperature of the heated component.

REFERENCES

Azar, K., and Moffat, R. J. (1991), Heat Transfer Coefficient and Its Estimation in Electronic Enclosures, Proceedings of the 1991 National Electronics Packaging and Production Conference (East), Boston, June 1991.

Fitch, J. S. (1990), A One-Dimensional Thermal Model for the VAX 9000 Multi-Chip Units, Thermal Modeling and Design of Electronic Systems and Devices, Presented at the Winter Annual Meeting of ASME, Dallas, November 1990.

Garimella, S. V. and Eibeck, P. A. (1990), Heat Transfer Characteristics of an Array of Protruding Elements in Single Phase Forced Convection, International Journal of Heat and Mass Transfer, vol. 33, no. 12, pp. 2659-2669.

Incropera, F. P. (1988), Convection Heat Transfer in Electronic Equipment Cooling, Journal of Heat Transfer, vol. 110, pp. 1097-1111.

Kang, B. H., Jaluria, Y., and Tewari, S. S. (1990), Mixed Convection Transport from an Isolated Heat Source Module on a Horizontal Plate, Journal of Heat Transfer, vol. 112, pp. 653-661.

Kline, S. J., and McClintock, F. A. (1953), Describing Uncertainties in Single-Sample Experiments, Mechanical Engineering, pp. 3-8.

Laderman, A. J., Osborn, D. B., Grabow, R. M., and Bury, M. C. (1987), Parametric Study of Conduction Cooling for High Power Density Electronics, Proceedings of the International Symposium of Electronic Technology for Electronic Equipment, Honolulu, March 1987.

Manno, V. P., and Azar, K. (1991), Impact of Heat Transfer Coefficient Models on the Simulation of Electronic Enclosure Thermal Response, Proceedings of the 1991 National Electronic Packaging and Production Conference (East), Boston, June 1991.

Ortega, A. (1986), Experiments on Buoyancy-Induced Convection Heat Transfer from an Array of Cubical Elements on a Vertical Channel Wall, Ph.D. Dissertation, Stanford University, June 1986.

Ortega, A., and Kabir, H. (1991), Substrate Conduction Mechanisms in Convectively Cooled Simulated Electronic Packages, Seventh IEEE Semi-Therm Symposium.

Roeller, P. T., Stevens, J., and Webb, B. W. (1990), Heat Transfer and Turbulent Flow Characteristics of Isolated Three Dimensional Protrusions in Channels, Thermal Modeling and Design of Electronic Systems and Devices, ASME HTD-vol. 153, pp. 7-13.

Wagner, G. R. (1984), "Circuit Board Material/Construction and its Effect on Thermal Management", Section 3, Chapter 2 in Thermal Management Concepts in Microelectronic Packaging: From Component to System, ISHM Technical Monograph Series 6984-003, S.S. Furkay, R.F. Kilburn and G. Monti, Editors, Published by the International Society for Hybrid Microelectronics, Silver Spring, MD.

Wang, Y., and Ghajar, A. J. (1991), Effect of Component Geometry and Layout on Flow Distribution for Surface Mounted Electronic Components: A Smoke Flow Visualization Study, Heat Transfer Enhancement in Electronics Cooling, eds. S. H. Bhavnani and M. Greiner, ASME, HTD-vol. 183, pp. 25-31.

Weiss, J., Fortner, P. Pearson, B., Watson, K. and Monroe, T. (1989), Modeling Air Flow in Electronic Packages, Mechanical Engineering, vol. 111, no. 9, pp. 56-58.